JPPIPA 11(5) (2025)

Jurnal Penelitian Pendidikan IPA

http://jppipa.unram.ac.id/index.php/jppipa/index

Improvement of Automatic Generation Control (AGC) with 2DOF-PID-PIID on Two Non-Reheat Turbine Areas in an Interconnected Power System

Rio Irawan[1*], Ermanu Azizul Hakim[1], Haneef Nouval Alannibras Humaidi[1]

[1] Electrical Engineering Department, Universitas Muhammadiyah Malang, Malang, Indonesia.

Received: January 13, 2025
Revised: March 30, 2025
Accepted: May 25, 2025
Published: May 31, 2025

Corresponding Author:
Ermanu Azizul Hakim
ermanu@umm.ac.id

DOI: 10.29303/jppipa.v11i5.11212

Abstract: An efficient and reliable electric power system must be able to maintain operational stability, especially in maintaining frequency stability to remain at its nominal value, both in constant conditions and when disturbances occur. For this reason, optimal frequency control is needed through Automatic Generation Control (AGC). In AGC, a controller is needed to accelerate the frequency response so that it is quickly stabilized. This study proposes the development of a 2DOF-PID controller into a 2DOF-PID-PIID optimized using the Dandelion Optimizer (DO) to improve AGC performance in the context of Load Frequency Control (LFC). The test results show that the DO algorithm gives better results compared to the Sine Cosine Algorithm (SCA), Pelican Optimization Algorithm (POA), and Archimedes Optimization Algorithm (AOA). Therefore, DO is chosen to optimize 2DOF-PID-PIID. The 2DOF-PID-PIID controller optimized with DO produces an ITAE (Integral Time Absolute Error) value of 0.001276, which is superior compared to the 2DOF-PID (0.00158), 2DOF-PID-PID (0.00158), PID (0.001833), and PIDD (0.002022) controllers, indicating its effectiveness in accelerating the response and maintaining frequency stability in the electric power system.

Keywords: Automatic generation control; Controller; Dandelion optimizer; Load frequency control (LFC); Optimization

Introduction

Electrical energy is very important for economic progress because it plays a role in driving industry, facilitating transportation, and supporting technological innovation (Doroodi et al., 2024). In an electric power system, there are several components that are interconnected before the energy finally reaches the user or consumer (Rashid et al., 2024). A reliable and efficient power system must be able to maintain its operational conditions, both in stable conditions and when disturbances occur. One important thing is the ability to maintain power stability between the power generated by the generator and the load requirements, including maintaining the frequency value at its nominal value (Khalid Saifullah et al., 2023). Frequency variations can have a negative impact on the generating system and also on the connected load, significant frequency deviations can cause collapse in the electric power system (Wadi et al., 2024). Therefore, maintaining a stable frequency at its nominal value is very important in the operation of the electric power system (Daraz et al., 2024; Vorobev et al., 2019). Changes in frequency and power imbalance, one of the causes of which is due to sudden changes in load, and this is a challenge that must be overcome (Geis-Schroer et al., 2024; Wang & Lu, 2024). Sudden load addition can slow down the generator rotation, resulting in a decrease in frequency (Liu et al., 2018). Conversely, sudden load removal will speed up the generator rotation and increase the

How to Cite:
Irawan, R., Hakim, E. A., & Humaidi, H. N. A. (2025). Improvement of Automatic Generation Control (AGC) with 2DOF-PID-PIID on Two Non-Reheat Turbine Areas in an Interconnected Power System. *Jurnal Penelitian Pendidikan IPA*, *11*(5), 233–246. https://doi.org/10.29303/jppipa.v11i5.11212

frequency value, thus affecting the frequency value (Li et al., 2024; Yang et al., 2022).

Controlling the frequency at the nominal value is very complex due to the ever-changing load variations (Khalil et al., 2024). Therefore, Automatic Generation Control (AGC) is needed to maintain frequency stability in the context of Load Frequency Control (LFC) (Zhou et al., 2024). To improve the performance of AGC to have a faster and more stable response, the use of an effective controller is required. One type of controller that is widely used is PID. PID controllers are controllers (Proportional Integral and Derivative). PID controllers have advantages because of their simple design and efficient cost-benefit ratio (Li, 2023). However, with the increasing complexity of the power system, PID controller alone is not optimal enough (Sahu et al., 2023). One innovative solution is to add Degrees of Freedom (DOF) which is effective in increasing the controller's ability to overcome load change disturbances (Chen & Luo, 2022). In previous studies, researchers have implemented various controllers, including Proportional-Integral-Derivative (PID) and variations of PID development with the addition of DOF or other types, for optimization in the context of load frequency control (LFC) in the electric power system. Such as Fractional-Order PID (FOPID) for Load Frequency Control (LFC) of the electric power system connected to the hydrogen energy storage unit (Illias et al., 2021; Verma et al., 2024).

Helmy showed the performance of the 2-DOF PID Controller in Automatic Generation Control (AGC) of two areas of the electric power system connected to each other using the Particle Swarm Optimization (PSO) algorithm. Furthermore, optimal performance was also shown in the PID controller in Automatic Generation Control for the two-area electric power system using Particle Swarm Optimization (PSO) (Karanam & Shaw, 2022). Then 2DOF-PID combined with PID or 2DOF PID-PID in automatic generation control (AGC) in the interconnected wind turbine electric power system gave very good results. 2DOF-IDD for AGC control on hybrid power system. Furthermore, proportional-Integral-Double Derivative (PIDD) on multi-area AGC gives good results. Another challenge is the sensitivity of the parameters on each controller, the parameters of each controller must be precise so that the controller can work optimally. Manual parameter search provides a big challenge considering the complexity of the controller structure and system involving many parameters (Fathy & Alharbi, 2021).

One solution is with a metaheuristic algorithm that is widely used in systems for Load Frequency Control (LFC). However, according to the "no free lunch" theory there is no single optimization technique that is always superior for all types of problems. Seeing this, it is important to use newer optimization algorithms and compare them with existing algorithms, as done in previous studies with similar system contexts, in order to achieve more optimal optimization results. Literature survey shows that the controller structure greatly affects the performance of AGC. Considering the excellent performance potential of the 2DOF-PID type controller, this study will develop a 2DOF-PID controller with a combination of a Proportional-Double Integral-Derivative (PIID) controller, namely a 2DOF-PID-PIID controller in the LFC system. Referring to the "no free lunch" theory (Gulzar et al., 2024), this study will also implement the Dandelion Optimizer (DO) metaheuristic algorithm, which is inspired by the movement of dandelion seeds (Zhao et al., 2022). The DO algorithm was chosen because in addition to being relatively new, several previous studies have shown that this method provides good results in the context of Load Frequency Control (LFC) and Automatic Generation Control (AGC) (Abdelkader et al., 2024; Elsawy Khalil et al., 2024).

In addition, we will also compare the DO algorithm with several other algorithms that have previously been applied in the context of Load Frequency Control, such as the Archimedes Optimization Algorithm (AOA), Pelican Optimization Algorithm (POA), and Sine Cosine Algorithm (SCA) which have previously been tested for their performance in the LFC context. Furthermore, the objective function selected as the system performance index is the Integral Time Absolute Error (ITAE). ITAE was chosen because it has good performance for the LFC objective, namely a fast stable response and minimizing peak deviations until reaching steady state conditions. In this study, the generating system used is a non-reheat steam power plant. The selection of a non-reheat steam turbine is based on its advantage in providing a faster response. In this study, there are two areas of steam turbines that are interconnected and have been integrated with the controller we proposed, namely 2DOF-PID-PIID.

The results of this controller are also compared with controllers that have been tested and provide good results in the context of LFC, such as PID controllers, PIDD, 2DOF PID and 2DOF-PID-PID. Thus, this study aims to introduce a controller structure that develops a 2DOF-PID controller into a 2DOF-PID-PIID, and evaluate its results on the implementation of Automatic Generation Control (AGC) of a two-area interconnected steam turbine power system. In addition, this study also aims to select the best optimization algorithm for AGC of a two-area interconnected power system on a non-reheat steam turbine, when disturbances such as load changes occur.

Method

System Modeling

In this study, we use a power system model with two interconnected non-reheat heat turbines, as depicted in Figure 1, based on an analysis framework adapted from previous research (Veerasamy et al., 2019). Each area consists of main components, namely governor, turbine, rotating mass & load and two controllers. The selection of non-reheat heat turbines is based on its advantages in providing faster response, and higher stability.

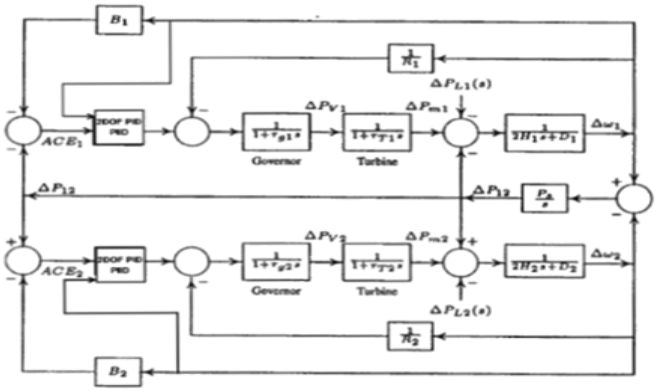

Figure 1. Modeling of non-reheat turbine system 2 areas that are interconnected and have integrated governor droop and controller

In this study, the transfer function of the non-reheat turbine unit is represented in equation (1).

$$G\ (s) = \frac{1}{1+sTt} \quad (1)$$

With T_t is the time-constant steam turbine non reheat. While the selected governor is the characteristic droop type because it can regulate the load difference more efficiently when several generators are connected to the same network compared to the Isochronous governor. The characteristic droop governor with steady-state feedback is equipped with a simplified speed reduction characteristic droop and has been represented in Figure 2.

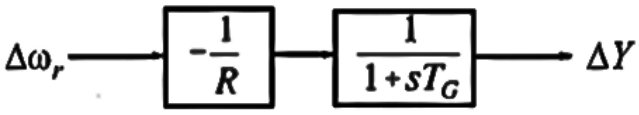

Figure 2. Governor speed droop

Here R is the speed droop regulation while T_Gs is the governor time constant, given the speed droop regulation and governor time constant values of 0.05 and 0.2s in area 1, and 0.0625 and 0.3 s in area 2. Then the rotating mass & load transfer function is represented in equation.

$$G\ (s) = \frac{1}{2H_S+D} \quad (2)$$

where H is constant inertia and D is constant damping, the constant inertia and constant damping values are 5 p.u and 0.6 p.u in area 1 while area 2 is given a value of 4 p.u and 0.9 p.u in area 2. In more detail, see table 1 for the Modeling parameters of the non-reheat turbine system 2 Areas that are interconnected and have integrated governor droop and controller

Table 1. Turbine System Parameters

Simbol	Name	Area 1	Area 2
R	Speed Regulation	0.05	0.0625
D	Coefficient	0.6	0.9
H	Inertia Constant	5	4
Tg	Governor Time Constant	0.2 s	0.3 s
Symbol	Name	Area 1	Area 2

Proposed Controller Design

In the context of conventional LFC (Load Frequency Control), the main objective is to set the ACE (Area Control Error) value for each area to zero. This control error is calculated through a linear combination of the frequency deviation and the tie-line error, which is described in equation (3).

$$ACE_i = \sum_{j=1}^{n} A_{Pj} + K_i \Delta\omega \quad (3)$$

System performance optimization is achieved when the Ki value is equalized with the connected area frequency bias factor, defined in equation (4).

$$B_i = \frac{1}{R_i+D_i} \quad (4)$$

Thus, ACE for a system with two areas is expressed by equations (5) and (6)

$$ACE_1 = \Delta P_{12} + B_1 \Delta\omega_1 \quad (5)$$

$$ACE_2 = \Delta P_{21} + B_2 \Delta\omega_2 \quad (6)$$

Where ΔP_12 and ΔP_21 are the deviations from the scheduled exchange, ACE is used as a driving signal to activate changes in the reference power set point, and when the steady-state condition is reached, ΔP_12 and Δω will be zero. Responding to the need for more optimal control in a variable 2-area power system, we propose a 2DOF-PID-PIID controller as a replacement for Ki to optimize the system response as seen in Figure 3.

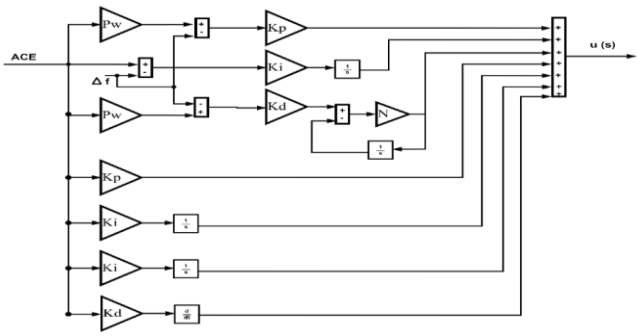

Figure 3. 2DOF-PID-PIID controller

From figure 3, the 2DOF – PID PIID controller is the result of the development of Two Degree Of Freedom PID (2 DOF PID) with the addition of one Proportional controller, 2 Integral Controllers and one derivative controller. By considering two inputs, ACE and Δf (frequency change), the output of the 2DOF-PID-PIID controller can be represented by the following equation.

$$U\ (s) = Kp\ \times A + \frac{Ki1}{s} \times B + \frac{Kd_s}{N.s+1} \times C + Kp\ \times Q + \frac{Ki2}{s} \times Q + \frac{Ki3}{s} + Q\ \times\ Kd_s +\ Q \quad (7)$$

where the values of A B C and Q are as follows

$$A = \{ACE\ (s) \times Pw -\ \Delta f\ (s)\} \quad (8)$$

$$B = \{ACE\ (s) -\ \Delta f\ (s)\} \quad (9)$$

$$C = \{ACE\ (s) \times Dw -\ \Delta f\ (s)\} \quad (10)$$

$$Q = ACE(s) \quad (11)$$

Objective Function

Objective function is a crucial indicator in evaluating the performance of a system to determine whether the system has been optimized or not. Specifically, the objective function is used to measure the level of error in the system. Therefore, a system is considered optimal when the error value or objective function value is as minimal as possible. In the context of 2DOF-PID-PIID controller optimization, the objective function value will be gradually minimized through each iteration. This process involves adjusting the combination of parameters in the 2DOF-PID-PIID controller carried out by the optimization algorithm to achieve maximum efficiency and the best performance of the system with the minimum error value. In the context of LFC, the main objective is to get a fast stable response and minimize the peak deviation to the state condition, therefore the ITAE (Integral Time Absolute Error) objective function is chosen with more optimal performance to support the two previous main objectives, because ITAE in the context of LFC shows better performance compared to IAE, ISE, and ITSE. In the mathematical model, ITAE is represented in equation (12).

$$ITAE = \int_0^{t_{sim}} (|\Delta f1| + |\Delta f2| + |\Delta P_{tie}|)\ \times t\ \times dt \quad (12)$$

Dandelion Optimizer

Dandelion Optimizer (DO) is an optimization algorithm inspired by the movement of dandelion seeds. This algorithm consists of three stages, namely rising, descending, and landing. In the rising stage, the seeds fly in a spiral due to wind eddies or float in groups according to weather conditions. In the descending stage, the flying seeds descend steadily, adjusting their direction in global space. In the landing stage, the seeds fall at random positions to grow. In the Dandelion Optimizer algorithm, each seed that falls during the landing process is the best solution. In the dandelion optimizer A is a random population where the optimization process begins, which is represented in the equation matrix (13).

$$A\ = \begin{bmatrix} x_1^1 & \cdots & x_1^{dim} \\ \vdots & \ddots & \vdots \\ x_{pop}^1 & \cdots & x_{pop}^{dim} \end{bmatrix} \quad (13)$$

where dim is the dimension of each solution in the search space, while pop is the population size, which indicates the number of candidate solutions in the optimization population. Then in DO each candidate solution is generated randomly between the upper bound (UB) and the lower bound (LB), with the i-th individual in Xi being calculated randomly using the rand function, which can be represented in equation (14).

$$x_i =\ x_{min} + rand\ (x_{max} -\ x_{min}) \quad (14)$$

where x_min is the lower bound (LB) and x_max is the upper bound (UB). Next, in the Dandelion Optimizer (DO), the best fitness value for each individual in the population will be calculated using equation (15), and to determine the elite solution, equation (16) is used. The solution with the best fitness value in DO is called the elite.

$$f_{best} = \min(f(x_i)) \quad (15)$$

$$x_{elite} =\ x\ (\ find(f_{best} ==\ f(x_i))) \quad (16)$$

Rising Stage

In the rising stage, Dandelion Optimizer (DO) adapts its strategy based on different weather conditions to optimize the solution search. In Condition 1, when the weather is sunny and windy, DO applies a lognormal distribution to the wind speed, which favors random exploration of dandelion seeds to different locations. In contrast, on rainy days, DO switches to local exploitation, focusing the search on improving the quality of existing solutions, without significant movement to new areas in the search space. When the weather is sunny and windy as condition 1, the equation used in the Dandelion Optimizer algorithm can be modeled as follows:

$$x_{t=1} = x_t + \alpha \times v_x \times v_y \times \ln Y \times (x_s - x_t) \quad (17)$$

$$x_s = rand\,(1, \dim) \times rand\,(x_{max} - x_{min}) + x_{min} \quad (18)$$

$$\ln Y = \begin{cases} \frac{1}{y\sqrt{2\pi}} \exp\left(-\frac{(\ln y)^2}{2\sigma^2}\right) & \text{if } y \geq 0 \\ 0 & \text{if } y < 0 \end{cases} \quad (19)$$

$$\alpha = \text{rand}() \times \left(\frac{1}{T^2}t^2 - \frac{2}{T}t + 1\right) \quad (20)$$

$$v_x = r \times \cos\,\theta \quad (21)$$

$$v_y = r \times \sin\,\theta \quad (22)$$

$$r = \frac{1}{e^{\theta}} \quad (23)$$

$$\theta = (2 \times \text{rand}() - 1) \times \pi \quad (24)$$

In sunny conditions, the wind speed follows a lognormal distribution (ln Y), and each dandelion seed is symbolized by x_t in the random search space x_s. The adaptive parameters that regulate the length of the dandelion's rising process are determined by α and the dandelion seed motion coefficients during the rising process, which are triggered by air eddies, are v_x and v_y. The direction of this movement is determined by the angle θ. While in rainy conditions as the second condition, the dandelion will exploit the local with the following mathematical equation,

$$x_{t=1} = x_t \times k \quad (25)$$

$$q = \frac{1}{T^2 - 2T + 1}t^2 - \frac{2}{T^2 - 2T + 1}t + 1 + \frac{1}{T^2 - 2T + 1} \quad (26)$$

$$k = 1 - \text{rand}() \times q \quad (27)$$

$$x_{t=1} = \begin{cases} x_t + \alpha \times v_x \times v_y \times \ln Y \times (x_s - x_t) & \text{randn} < 1.5 \\ x_t \times k & \text{else} \end{cases} \quad (28)$$

k is used to maintain the local search area of an agent, while randn is a function that generates random values according to the standard normal distribution.

Descending Stage

At this stage, the dandelion seed will continue to decline after reaching a peak in the rising phase at a certain value. The seed will continue to adjust its direction in the global space to adapt to changing conditions. The mathematical modeling for this phase is described as follows:

$$x_{t=1} = x_t - \alpha \times \beta_t \times \left(x_{\text{mean\_t}} - \alpha \times \beta_t \times x_t\right) \quad (29)$$

$$x_{\text{mean\_t}} = \frac{1}{\text{pop}} \sum_{i=1}^{pop} x_i \quad (30)$$

where α is an adaptive parameter that adjusts the stride length in the movement of dandelion seeds, while β_t represents the Brownian action and is a random value derived from a standard normal distribution.

Landing Stage

In this phase, the landing location of the dandelion seeds is determined randomly, with the best position being used as the optimal solution. Information from elite dandelion seeds, which have the highest fitness value, is exploited locally to achieve optimal global accuracy, the mathematical model of this phase is represented as follows:

$$x_{t=1} = x_{\text{elite}} + \text{levy}(\lambda) \times \alpha \times (x_{\text{elite}} - x_t \times \delta) \quad (31)$$

$$\text{levy}(\lambda) = s\frac{\omega \times \sigma}{|t|^{\frac{1}{\beta}}} \quad (32)$$

$$\sigma = \left(\frac{\Gamma(1+\beta) \times \sin\left(\frac{\pi\beta}{2}\right)}{\Gamma\left(\frac{1+\beta}{2}\right) \times \beta \times 2^{\left(\frac{\beta-1}{2}\right)}}\right) \quad (33)$$

$$\delta = \frac{2t}{T} \quad (34)$$

x_{elite} is the best position of the agent at each iteration and levy(λ) is the function of levy flight

Table 2. DO Parameters Used During Simulation

Parameter	Mark
Number of Search Agents	15
Maximum Number of Iterations	50
Upper Bound	10
Lower Bound	-10

Result and Discussion

Before testing each controller, we will assess the performance of the optimization method by comparing the dandelion optimizer (DO) with other optimization methods including (AOA) (Hemeida et al., 2022; Al Hwaitat et al., 2025), (AGTO), (POA) (Debbarma et al., 2024), (SCA) (Iqbal et al., 2024). The system model in Figure 1 has then been implemented for testing in MATLAB-Simulink. For testing, we provide a Step Load Perturbation (SLP) of 0.1 pu in all areas, and DO optimization is carried out for 50 iterations with a population size of 15. The results of the optimizer performance comparison can be seen in Table 3.

From table 3 it can be seen that DO has better performance than other optimizers. Therefore DO is chosen to perform tuning on each proposed controller. Next we tested by comparing 6 controllers that were previously tested in the LFC context including PID (Nassef et al., 2023), PIDD (Sahu et al., 2016), FOPID (Barakat, 2022), 2DOF PID [40], 2DOF-PID-PID [42], With the controller we proposed, namely 2DOF-PID-PIID to see the best performance of each controller, which is optimized with Dandelion Optimizer (DO). From the test results with Step Load Perturbation (SLP) 0.1 pu in all areas, and DO optimization was carried out for 50 iterations with a population size of 15, the parameters in table 4 were obtained for area 1 and table 5 for area 2.

Table 3. Comparison of Optimization Methods

Iterasi	Optimizer	Controller	ITAE
50	Dandelion Optimizer (DO)	2DOF-PID-PIID	0.001276
50	Sine Cosine Algorithm (SCA)		0.002153
50	Pelican Optimization Algoritm (POA)		0.002902
50	Archimedes Optimization Algorithm (AOA)		0.005200

Table 4. Controller Parameters with DO Area 1 Optimization

Parameters								Area Controller Parameters 2		
Dandelion Optimizer	Kp	Ki	Kd	Pw	Dw	Kp2	Ki2	Ki3	Kd2	Kd3
2DOF-PID-PIID	2.0414	-0.4956	-5.2802	-9.6232	-9.6918	9.8511	0.1395	9.8705	0.9867	
2DOF-PID-PID	2.2906	8.6529	1.3501	3.8416	2.7469	-0.7663	10	-	-0.0776	
2DOF-PID	-9.5975	-8.6104	-6.3336	-1.8497	-8.8152	-	-	-	-	
PIDD	7.6907	6.3122	0.8619	-	-	-	-	-	3.2229	
PID	6.4980	6.7159	2.7189	-	-	-	-	-	-	

Table 5. Controller Parameters with DO Area 1 Optimization

Parameters								Area Controller Parameters 2		
Dandelion Optimizer	Kp	Ki	Kd	Pw	Dw	Kp2	Ki2	Ki3	Kd2	Kd3
2DOF-PID-PIID	-0.9177	2.8065	-0.52562	8.7543	4.9306	8.7688	6.1063	9.5672	5.7749	
2DOF-PID-PID	-7.0948	-0.1285	0.9972	-4.0684	0.1088	5.4684	9.8220		7.47047	
2DOF-PID	-9.0846	-9.8584	-4.9054	2.2526	4.0233					
PIDD	10	7.3511	5.2988						1.2746	
PID	7.8185	7.76589	4.55612							

All parameters obtained in Table 4 and Table 5 by providing Step Load Perturbation (SLP) of 0.1 pu. From the test results, it was obtained that the 2DOF-PID-PIID controller showed very good performance with the smallest ITAE (Integral Time Absolute Error) value, which was 0.001276. This value indicates that the 2DOF-PID-PIID controller has better performance compared to other controllers in the context of Load Frequency Control (LFC), especially in providing a faster and more effective frequency response to return to steady state after disturbances in the form of load changes or SLP (Patel et al., 2018). This controller is able to reduce errors optimally, which means it can regulate the frequency more accurately and stably. The ITAE results of all controllers can refer to table 6.

Table 6. Comparison of Best Fitness in the form of ITAE for Each Controller

Controller	ITAE
2DOF-PID-PIID	0.001276
2DOF-PID	0.00158
2DOF-PID-PID	0.00158

Controller	ITAE
PID	0.001833
PIDD	0.002022

Table 7. Comparison of Settling Time Overshot and Undershot Frequency Deviation Scenario 1 Area 1

Controller	Settling Time (sec)	Overshot (Hz)	Undershot (Hz)
2DOF-PID-PIID	4.96	0.000114	0.001289
2DOF-PID	5.742	0.0000993	0.001341
2DOF-PID-PID	5.74	0.0000833	0.001311
PID	5.92	0.000033	0.00156
PIDD	8.4	0.00000321	0.00122

In Table 7, the 2DOF-PID-PIID controller shows superiority in managing frequency deviation in Area 1, especially in terms of settling time which is only 4.96 seconds. This indicates a faster and more effective response compared to other controllers reviewed, such as 2DOF-PID, 2DOF-PID-PID, PID, and PIDD, all of which have longer settling times. In addition, 2DOF-PID-PIID also shows improvement in reducing undershoot, with lower values compared to 2DOF-PID and PID controllers. Although PIDD recorded the lowest undershoot value, this controller had a relatively high settling time (8.4 seconds), which may be undesirable in applications that require fast response. Although 2DOF-PID-PIID did not have the lowest overshoot and undershoot values in absolute terms, the difference in these values was relatively small when compared to other controllers. The results of the frequency deviation plot or ΔF for Area 1 in scenario 1 can be seen in Figure 4, which provides a clear visualization of the performance of the 2DOF-PID-PIID controller in regulating frequency compared to other controllers.

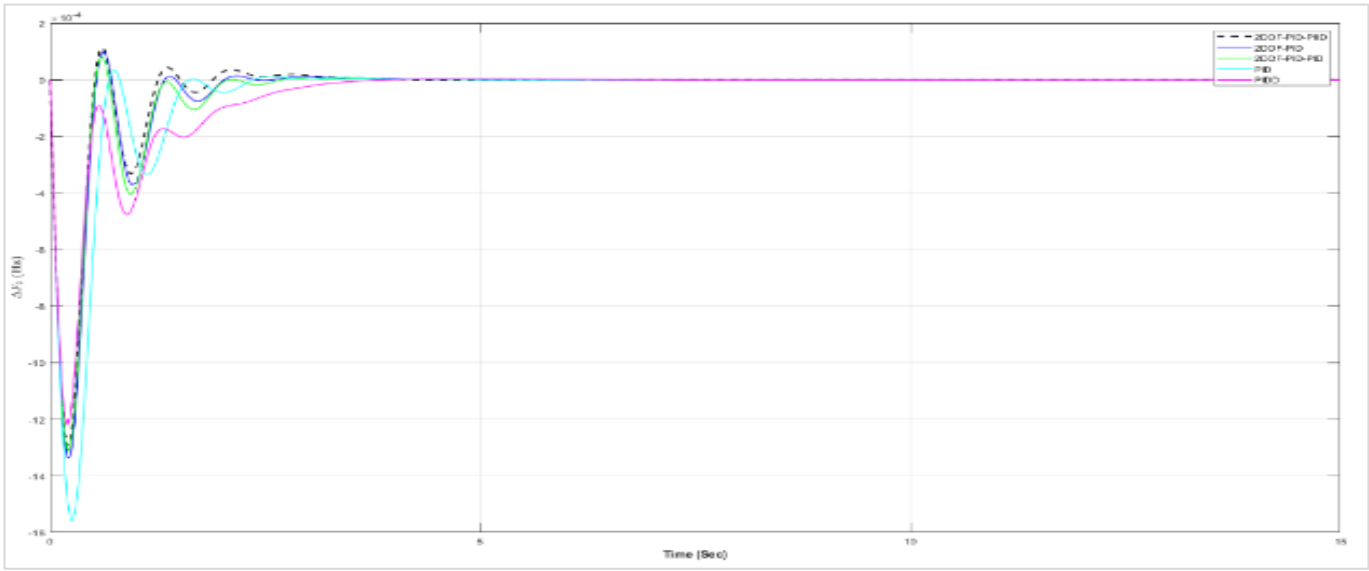

Figure 4. Frequency deviation of scenario 1 in area 1

Furthermore, in managing the frequency deviation (Δf) in Area 2, the 2DOF-PID-PIID controller again shows superior performance compared to other controllers. Detailed comparisons regarding settling time, overshoot, and undershoot for Area 2 can be found in Table 8.

Table 8. Comparison of Settling Time Overshot and Undershot Frequency Deviation of Scenario 1 Area 2

Controller	Settling Time (sec)	Overshot (Hz)	Undershot (Hz)
2DOF-PID-PIID	7.01	0.0003924	0.001528
2DOF-PID	8.041	0.0003845	0.001657
2DOF-PID-PID	7.79	0.0003739	0.001608
PID	8.54	0.000327	0.00192
PIDD	8.42	0.0002737	0.001585

Table 8 shows the performance comparison of the 2DOF-PID-PIID controller against other controllers in handling frequency deviation (Δf) in Area 2 in scenario 1. The 2DOF-PID-PIID controller successfully achieved a faster settling time of 7.01 seconds, indicating a more efficient response compared to the 2DOF-PID, 2DOF-PID-PID, PID, and PIDD controllers which recorded settling times of 8.041 seconds, 7.79 seconds, 8.54 seconds, and 8.42 seconds, respectively. In addition, in terms of reducing undershoot, the 2DOF-PID-PIID also showed the most superior performance with the lowest value of 0.001528 Hz, lower than the other controllers. As for overshoot, although PIDD shows the lowest value, at 0.0002737 Hz, this controller also has a longer settling time, at 8.42 seconds, indicating a trade-off between overshoot accuracy and response speed. For a clearer visualization of the performance of this controller

in handling frequency deviation in Area 2 for the second scenario, see Figure 5.

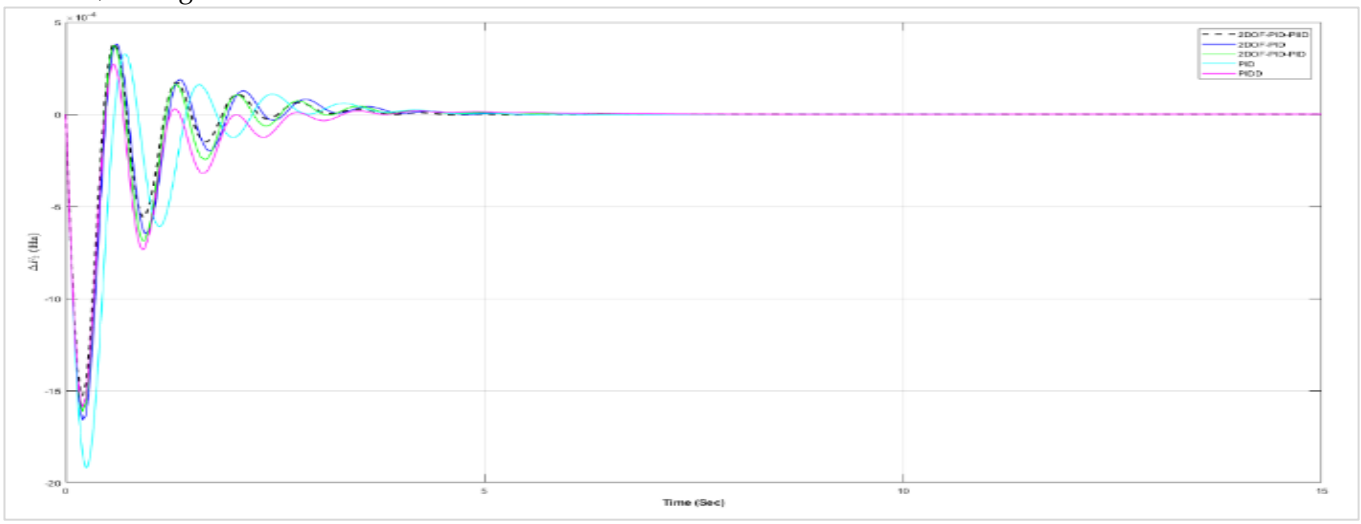

Figure 5. FD at Area 2 SLP 0.1 Pu in All Areas

From the data analysis presented in Table 9, it can be seen that the performance difference between the 2DOF-PID-PIID, 2DOF-PID, and 2DOF-PID-PID controllers is quite small, indicating similar efficiency in managing Ptie deviation for all areas. However, the 2DOF-PID-PIID controller stands out with the fastest settling time of 8.11 seconds, indicating its superior ability to achieve stability faster than other controllers. In addition, this controller also recorded a relatively low overshoot value of 0.000106 Hz and an undershoot of 0.0000538 Hz, indicating a good balance between response speed and output fluctuation control. To validate the performance in managing the Ptie delta, the researcher performed a special ITAE calculation for the Ptie output as additional validation, considering the very small difference in this component. Different from the previously reported overall ITAE calculations, a special focus on the Ptie output error yields the smallest ITAE value in 2DOF-PID-PIID with 0.000397, strengthening the evidence that this controller is effective in reducing the absolute error and offering optimal response.

Table 9. Comparison of Settling Time Overshot and Undershot ΔPtie Scenario 1 All Areas

Controller	Settling Time (sec)	Overshot (Hz)	Undershot (Hz)	ITAE Ptie
2DOF-PID-PIID	8.11	0.000106	0.0000538	0.000397
2DOF-PID	8.23	0.0001615	0.00000658	0.000483
2DOF-PID-PID	8.4	0.000141	0.00000416	0.000481
PID	9.21	0.000210	0.00000644	0.000536
PID	9.19	0.0001813	0	0.000486

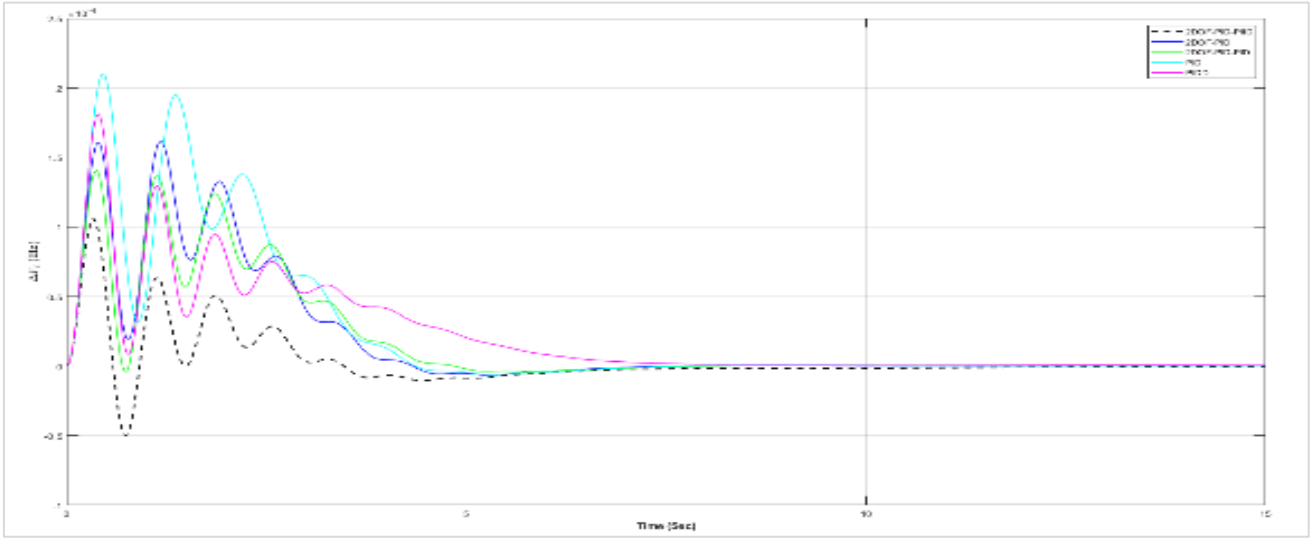

Figure 6. Delta Ptie In Scenario 1 SLP 0.1 in all areas

In Figure 6, the visualization of Δ Ptie clearly shows the superiority of the 2DOF-PID-PIID controller in managing deviations from the set point value. Although the difference in settling time between the controllers is relatively small, the resulting curves show that the 2DOF-PID-PIID successfully maintains a lower deviation throughout the system response. This decrease in signal fluctuations not only indicates a stable response but also directly contributes to the lower ITAE value. ITAE, which measures the total absolute error accumulated over time, becomes smaller as a result of the reduction in the amplitude of these fluctuations. Therefore, the effectiveness of the 2DOF-PID-PIID in minimizing errors not only improves the stability but also the overall efficiency of the system.

Scenario 2

In this second scenario, we will evaluate the performance of the various controllers by imposing a larger Step Load Perturbation (SLP) than in the previous test. Specifically, the SLP will be applied at 0.2 pu in Area 1 and -0.1 pu in Area 2. The purpose of this approach is to observe the controllers' response to significant changes in SLP and assess their effectiveness in managing more extreme frequency deviations. This testing is important to determine the ability of each controller to handle more challenging operational conditions.

From the results of the second scenario test, the ITAE values of all controllers show very significant differences under more extreme conditions. The best performance is shown by the 2DOF-PID-PIID controller with the lowest ITAE value of 0.01493, indicating the highest efficiency in reducing accumulated errors throughout the response time. Followed by 2DOF-PID-PID (Y. Li et al., 2024; So, 2022; Joseph et al., 2022) with an ITAE value of 0.01848, which shows an increase in performance compared to 2DOF-PID (Shahi et al., 2024; Roy et al., 2021; So, 2021), which recorded an ITAE value of 0.01853. Under larger SLP conditions, 2DOF-PID-PID is proven to be more effective than 2DOF-PID. The controller performance is then ranked by PID which recorded an ITAE value of 0.02354, and finally PIDD with a value of 0.02521.

Table 10. ITAE Comparison of Scenario 2

Controller	ITAE
2DOF-PID-PIID	0.01493
2DOF-PID-PID	0.01848
2DOF-PID	0.01853
PID	0.02354
PIDD	0.02521

Table 11. Comparison of Settling Time, Overshoot, and Undershoot ΔF Area 1 Scenario 2

Controller	Settling Time (sec)	Overshot (Hz)	Undershot (Hz)
2DOF-PID-PIID	14.80	0.0004439	0.002553
2DOF-PID	17.60	0.0004731	0.002642
2DOF-PID-PID	17.50	0.00034	0.002593
PID	15.90	0.0003239	0.003053
PIDD	20.07	0.0001205	0.002422

Table 11 shows a comparison of the performance of area 1 frequency deviation in scenario 2 for each controller in terms of settling time, overshoot, and undershoot.

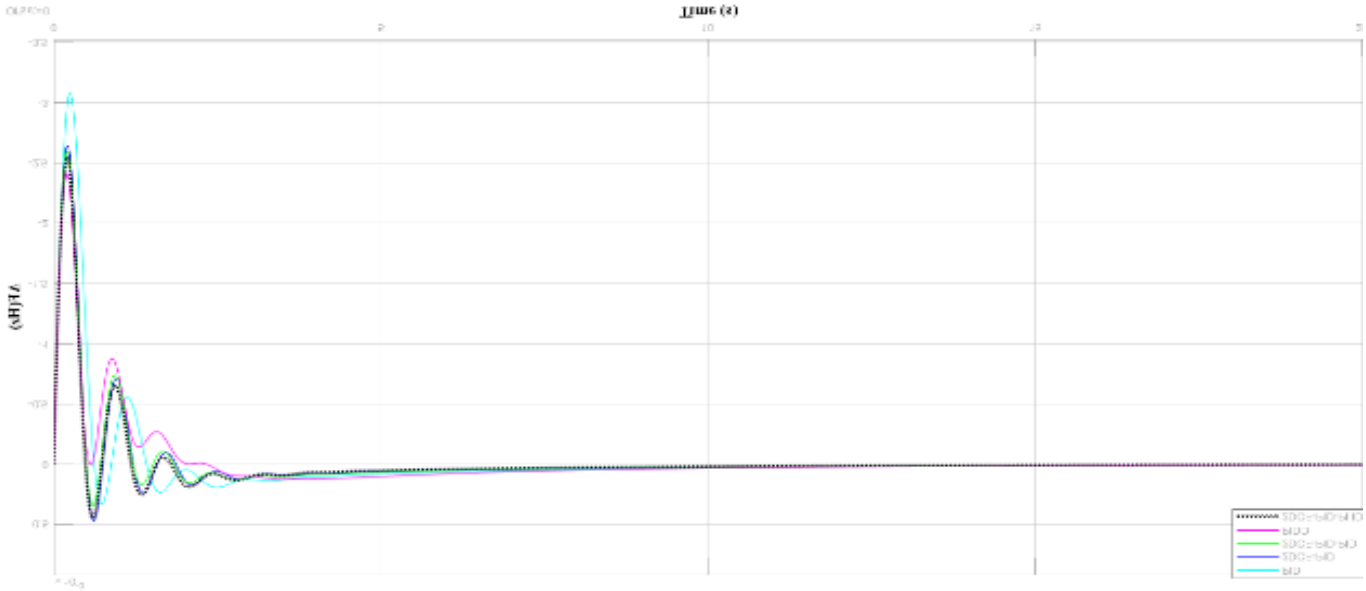

Figure 7. ΔF area 1 scenario 2

Table 11 provides a comparison of the controller performance in terms of settling time, overshoot, and undershoot for frequency deviation in Area 1 in the second scenario. The 2DOF-PID-PIID controller stands out with impressive performance, recording the fastest settling time of only 14.8 seconds, faster than the other controllers. In terms of undershoot, this controller also shows excellent results, with lower values compared to 2DOF-PID (Ogar et al., 2023; Huba et al., 2025), 2DOF-PID-PID (Appasani et al., 2023; Desalegn et al., 2022) and PID (Mohapatra et al., 2020). Although PIDD (Mosca et al., 2019; Jian et al., 2021) recorded the lowest undershoot value of 0.002422, it had the longest settling time of 20.07 seconds. Overall, 2DOF-PID-PIID is considered superior even though it does not have the lowest undershoot and overshoot values. The difference in values is very small compared to the much faster settling time compared to the other controllers. This shows a good balance between adaptation speed and stability in the face of more significant frequency deviations (Shrestha & Gonzalez-Longatt, 2021; Muftić Dedović et al., 2024; (Radaelli & Martinez, 2022; Rajak & Pudur, 2025). Visualization of the frequency deviation of Area 1 in this scenario can be seen further in Figure 7.

Table 12. Comparison of Settling Time, Overshoot, and Undershoot ΔF Area 1 Scenario 2

Controller	Settling Time (sec)	Overshot (Hz)	Undershot (Hz)
2DOF-PID-PIID	18.10	0.001511	0.000590
2DOF-PID	21.1	0.001635	0.000560
2DOF-PID-PID	19.53	0.001591	0.000588
PID	21.3	0.001884	0.0006183
PIDD	22.83	0.001568	0.0004632

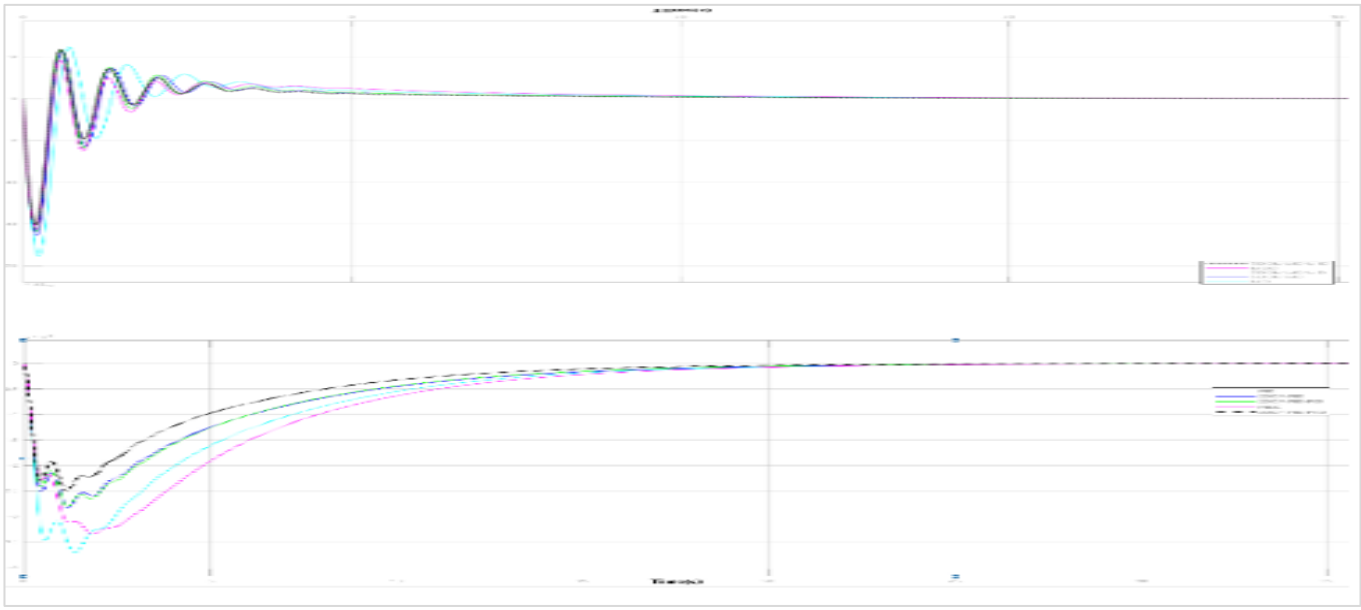

Figure 8. ΔF area 2 in the second scenario

Table 12 shows the results of the frequency deviation test in the second scenario for Area 2, where the 2DOF-PID-PIID controller demonstrates superior performance in several key aspects. With a settling time of only 18.10 seconds, this controller not only stabilizes the frequency the fastest among all controllers tested but also successfully suppresses overshoot with a relatively low value of 0.001511 Hz. The 2DOF-PID-PIID controller also recorded an undershoot value of 0.000590 Hz, lower than the PID controller, indicating a balance between fast response and precise control. Although PIDD achieved the lowest undershoot value (0.0004632 Hz), its longer settling time (22.83 seconds) indicates that there is a trade-off between response speed and stability. Furthermore, a visualization of the frequency deviation for the second scenario in Area 2 can be seen in Figure 8, which visually compares the performance of all controllers, showing how each handles more challenging conditions.

Table 13. Comparison of Settling Time, Overshoot, and Undershoot in ΔPtie Scenario 2

Controller	Settling Time (sec)	Overshot (Hz)	Undershot (Hz)
2DOF-PID-PIID	29.08	0	0.002506
2DOF-PID [40]	33.32	0	0.002834
2DOF-PID-PID [42]	32.01	0	0.002818
PID [41]	32.98	0	0.002836
PIDD [44]	31.46	0	0.003342

Table 13 shows the test results of ΔPtie in all areas in the second scenario, comparing the settling time, overshoot, and undershoot between controllers. The

2DOF-PID-PIID controller shows superior performance with the fastest settling time of 29.08 seconds, indicating a more responsive response compared to other controllers. In addition, 2DOF-PID-PIID also recorded the lowest undershoot value among all controllers with 0.002506 p.u., confirming its effectiveness in limiting fluctuations below the set point without causing overshoot. A detailed visualization of ΔPtie in this scenario can be seen in Figure 9, which clearly illustrates the superior performance of 2DOF-PID-PIID compared to other controllers under the same test conditions.

Conclusion

From a series of tests conducted in various scenarios, the 2DOF-PID-PIID controller consistently shows superior performance compared to other controllers. Especially in the second scenario, in the ΔPtie test in all areas, the 2DOF-PID-PIID not only recorded the fastest settling time, but also managed to maintain the lowest undershoot value. This shows its superior ability to manage frequency fluctuations with high efficiency and stability. This test confirms that the development of 2DOF-PID to 2DOF-PID-PIID provides significant advantages in handling greater variability in load or sudden changes in the system. In the context of Load Frequency Control (LFC), this controller shows great potential in handling frequency deviations. Further developments have the opportunity to test this controller in more complex systems, such as electric power systems consisting of four or more areas, with diverse sources including renewable energy sources (RES) and integrated Electric Vehicles (EV). This trial can provide further insight into the adaptability and scalability of the 2DOF-PID-PIID controller in facing more dynamic and diverse operational challenges.

Acknowledgments
Thanks to all parties who have supported the implementation of this research. I hope this research can be useful.

Author Contributions
Conceptualization, R. I.; methodology, E. A. H.; validation, H. N. A. H.; formal analysis, R. I.; investigation, E. A. H.; resources, H. N. A. H.; data curation, E. A. H.: writing—original draft preparation, R. I.; writing—review and editing, P. M. Z.: visualization, H. N. A. H. All authors have read and agreed to the published version of the manuscript.

Funding
Researchers independently funded this research.

Conflicts of Interest
The authors declare no conflict of interest.

References

Abdelkader, A. E., Magdy, G., Elhady, B., Ahmed, A. E., & Mansour, N. M. (2024). Dandelion Optimizer-Based Frequency Controller for a Hybrid power systems Considering Renewables. *Suez Canal Engineering, Energy and Environmental Science*, *2*(2), 8–16. https://doi.org/10.21608/sceee.2024.294718.1031

Al Hwaitat, A. K., Fakhouri, H. N., Zraqou, J., & Sirhan, N. (2025). Hybrid Optimization Algorithm for Solving Attack-Response Optimization and Engineering Design Problems. *Algorithms*, *18*(3), 160. https://doi.org/10.3390/a18030160

Appasani, B., Jha, A. V., Gupta, D. K., Bizon, N., & Thounthong, P. (2023). PSOα: A Fragmented Swarm Optimisation for Improved Load Frequency Control of a Hybrid Power System Using FOPID. *Energies*, *16*(5), 2226. https://doi.org/10.3390/en16052226

Barakat, M. (2022). Optimal design of fuzzy-PID controller for automatic generation control of multi-source interconnected power system. *Neural Computing and Applications*, *34*(21), 18859–18880. https://doi.org/10.1007/s00521-022-07470-4

Chen, P., & Luo, Y. (2022). A Two-Degree-of-Freedom Controller Design Satisfying Separation Principle With Fractional-Order PD and Generalized ESO. *IEEE/ASME Transactions on Mechatronics*, *27*(1), 137–148. https://doi.org/10.1109/TMECH.2021.3059160

Daraz, A., Alrajhi, H., Alahmadi, A. N. M., Bajaj, M., Afzal, A. R., Zhang, G., & Xu, K. (2024). Frequency stabilization of interconnected diverse power systems with integration of renewable energies and energy storage systems. *Scientific Reports*, *14*(1), 25655. https://doi.org/10.1038/s41598-024-76980-z

Debbarma, L., Debbarma, S., Roy, K., Roy, S. D., & Singh, P. P. (2024). Joint contribution of RTEM and AGC system for frequency stabilisation in renewable energy integrated power system. *IET Energy Systems Integration*, *6*(4), 498–511. https://doi.org/10.1049/esi2.12145

Desalegn, B., Gebeyehu, D., & Tamrat, B. (2022). Evaluating the performances of PI controller (2DOF) under linear and nonlinear operations of DFIG-based WECS: A simulation study. *Heliyon*, *8*(12), e11912. https://doi.org/10.1016/j.heliyon.2022.e11912

Doroodi, M., Ostadi, B., Husseinzadeh Kashan, A., & Zegordi, S. H. (2024). A hybrid method of system dynamics and design of experiments for investigating the economic and environmental

indicators of electricity industry. *Heliyon*, *10*(11), e31260. https://doi.org/10.1016/j.heliyon.2024.e31260

Elsawy Khalil, A., Boghdady, T. A., Alham, M. H., & Ibrahim, D. K. (2024). A novel cascade-loop controller for load frequency control of isolated microgrid via dandelion optimizer. *Ain Shams Engineering Journal*, *15*(3), 102526. https://doi.org/10.1016/j.asej.2023.102526

Fathy, A., & Alharbi, A. G. (2021). Recent Approach Based Movable Damped Wave Algorithm for Designing Fractional-Order PID Load Frequency Control Installed in Multi-Interconnected Plants With Renewable Energy. *IEEE Access*, *9*, 71072–71089. https://doi.org/10.1109/ACCESS.2021.3078825

Geis-Schroer, J., Tao, Q., Courcelle, M., Bock, G., Suriyah, M., Leibfried, T., & Carne, G. D. (2024). Power-to-Frequency Dependency of Residential Loads in a Wider Frequency Range: An Experimental Investigation. *IEEE Transactions on Industry Applications*, *60*(6), 9184–9194. https://doi.org/10.1109/TIA.2024.3439498

Gulzar, M. M., Sibtain, D., Al-Dhaifallah, M., Alismail, F., & Khalid, M. (2024). A new optimal 3° of freedom fractional order proportion integral derivative controller with model predictive controller for frequency regulation in high penetrated renewable based interconnected system. *Computers and Electrical Engineering*, *119*, 109651. https://doi.org/10.1016/j.compeleceng.2024.109651

Hemeida, M. G., Osheba, D. S., Senjyu, T., & Roshdy, M. (2022). Archimedes optimization algorithm based PI Controller for a two area Load Frequency Control. *2022 23rd International Middle East Power Systems Conference (MEPCON)*, 1–7. https://doi.org/10.1109/MEPCON55441.2022.10021764

Huba, M., Bistak, P., Vrancic, D., & Sun, M. (2025). PID vs. Model-Based Control for the Double Integrator Plus Dead-Time Model: Noise Attenuation and Robustness Aspects. *Mathematics*, *13*(4), 664. https://doi.org/10.3390/math13040664

Illias, H. A., Nurjannah, N., & Mokhlis, H. (2021). Optimal Performance of Automatic Generation Control for Two-Area Power System using Particle Swarm Optimization. *2021 Innovations in Power and Advanced Computing Technologies (i-PACT)*, 1–5. https://doi.org/10.1109/i-PACT52855.2021.9696446

Iqbal, M. S., Limon, Md. F. A., Kabir, Md. M., Rabby, M. K. M., Soeb, Md. J. A., & Jubayer, Md. F. (2024). A hybrid optimization algorithm for improving load frequency control in interconnected power systems. *Expert Systems with Applications*, *249*, 123702. https://doi.org/10.1016/j.eswa.2024.123702

Jian, Y., Lei, W., & Xingwang, Z. (2021). A Model-Driven Two-Degree-of-Freedom PID Controller with Manual/Automatic Switching Without Disturbance. *Journal of Physics: Conference Series*, *2005*(1), 012197. https://doi.org/10.1088/1742-6596/2005/1/012197

Joseph, S. B., Dada, E. G., Abidemi, A., Oyewola, D. O., & Khammas, B. M. (2022). Metaheuristic algorithms for PID controller parameters tuning: Review, approaches and open problems. *Heliyon*, *8*(5), e09399. https://doi.org/10.1016/j.heliyon.2022.e09399

Karanam, A. N., & Shaw, B. (2022). A new two-degree of freedom combined PID controller for automatic generation control of a wind integrated interconnected power system. *Protection and Control of Modern Power Systems*, *7*(1), 20. https://doi.org/10.1186/s41601-022-00241-2

Khalid Saifullah, M., Monirul Kabir, Md., & Rafiqul Islam, K. (2023). Improvement of voltage stability and loadability of power system employing the placement of unified power flow controller using artificial neural network. *International Journal of Electrical and Computer Engineering (IJECE)*, *13*(5), 4868. https://doi.org/10.11591/ijece.v13i5.pp4868-4877

Khalil, A. E., Boghdady, T. A., Alham, M. H., & Ibrahim, D. K. (2024). A novel multi-objective tuning formula for load frequency controllers in an isolated low-inertia microgrid incorporating PV/wind/FC/BESS. *Journal of Energy Storage*, *82*, 110606. https://doi.org/10.1016/j.est.2024.110606

Li, X., Wang, W., Ye, L., Ren, G., Fang, F., Liu, J., Chen, Z., & Zhou, Q. (2024). Improving frequency regulation ability for a wind-thermal power system by multi-objective optimized sliding mode control design. *Energy*, *300*, 131535. https://doi.org/10.1016/j.energy.2024.131535

Li, Y., Cao, J., Xu, Y., Zhu, L., & Dong, Z. Y. (2024). Deep learning based on Transformer architecture for power system short-term voltage stability assessment with class imbalance. *Renewable and Sustainable Energy Reviews*, *189*, 113913. https://doi.org/10.1016/j.rser.2023.113913

Li, Z. (2023). Review of PID control design and tuning methods. *Journal of Physics: Conference Series*, *2649*(1), 012009. https://doi.org/10.1088/1742-6596/2649/1/012009

Liu, K., Qu, Y., Kim, H.-M., & Song, H. (2018). Avoiding Frequency Second Dip in Power Unreserved Control During Wind Power Rotational Speed

Recovery. *IEEE Transactions on Power Systems*, *33*(3), 3097–3106. https://doi.org/10.1109/TPWRS.2017.2761897

Mohapatra, S., Sahu, P. C., Agrawal, R., Prusty, R. C., & Patel, N. C. (2020). Superiority of JAYA Optimized 2DOF-IDD control strategy for AGC of hybrid power system. *International Conference on Computational Intelligence for Smart Power System and Sustainable Energy (CISPSSE)*, 1–6. https://doi.org/10.1109/CISPSSE49931.2020.9212293

Mosca, C., Arrigo, F., Mazza, A., Bompard, E., Carpaneto, E., Chicco, G., & Cuccia, P. (2019). Mitigation of frequency stability issues in low inertia power systems using synchronous compensators and battery energy storage systems. *IET Generation, Transmission & Distribution*, *13*(17), 3951–3959. https://doi.org/10.1049/iet-gtd.2018.7008

Muftić Dedović, M., Avdaković, S., Musić, M., & Kuzle, I. (2024). Enhancing power system stability with adaptive under frequency load shedding using synchrophasor measurements and empirical mode decomposition. *International Journal of Electrical Power & Energy Systems*, *160*, 110133. https://doi.org/10.1016/j.ijepes.2024.110133

Nassef, A. M., Abdelkareem, M. A., Maghrabie, H. M., & Baroutaji, A. (2023). Review of Metaheuristic Optimization Algorithms for Power Systems Problems. *Sustainability*, *15*(12), 9434. https://doi.org/10.3390/su15129434

Ogar, V. N., Hussain, S., & Gamage, K. A. A. (2023). Load Frequency Control Using the Particle Swarm Optimisation Algorithm and PID Controller for Effective Monitoring of Transmission Line. *Energies*, *16*(15), 5748. https://doi.org/10.3390/en16155748

Patel, R. R., Awan, S. N., Barkmeier-Kraemer, J., Courey, M., Deliyski, D., Eadie, T., Paul, D., Švec, J. G., & Hillman, R. (2018). Recommended Protocols for Instrumental Assessment of Voice: American Speech-Language-Hearing Association Expert Panel to Develop a Protocol for Instrumental Assessment of Vocal Function. *American Journal of Speech-Language Pathology*, *27*(3), 887–905. https://doi.org/10.1044/2018_AJSLP-17-0009

Radaelli, L., & Martinez, S. (2022). Frequency Stability Analysis of a Low Inertia Power System with Interactions among Power Electronics Interfaced Generators with Frequency Response Capabilities. *Applied Sciences*, *12*(21), 11126. https://doi.org/10.3390/app122111126

Rajak, M. K., & Pudur, R. (2025). Multiobjective adaptive predictive virtual synchronous generator control strategy for grid stability and renewable integration. *Scientific Reports*, *15*(1), 9241. https://doi.org/10.1038/s41598-025-93721-y

Rashid, M. H., Abed, N. Y., Hussien, Z. F., Rahim, A. A., & Abdullah, N. (2024). Electric Power System. In *Power Electronics Handbook*. Elsevier. https://doi.org/10.1016/B978-0-323-99216-9.00009-3

Roy, R., Islam, M., Rashid, M., Mounis, S., Ahsan, M. M., Ahad, M. T., Siddique, Z., Kouzani, A. Z., & Mahmud, M. A. P. (2021). Investigation of 2DOF PID Controller for Physio-Therapeutic Application for Elbow Rehabilitation. *Applied Sciences*, *11*(18), 8617. https://doi.org/10.3390/app11188617

Sahu, P. R., Simhadri, K., Mohanty, B., Hota, P. K., Abdelaziz, A. Y., Albalawi, F., Ghoneim, S. S. M., & Elsisi, M. (2023). Effective Load Frequency Control of Power System with Two-Degree Freedom Tilt-Integral-Derivative Based on Whale Optimization Algorithm. *Sustainability*, *15*(2), 1515. https://doi.org/10.3390/su15021515

Sahu, R. K., Gorripotu, T. S., & Panda, S. (2016). Automatic generation control of multi-area power systems with diverse energy sources using Teaching Learning Based Optimization algorithm. *Engineering Science and Technology, an International Journal*, *19*(1), 113–134. https://doi.org/10.1016/j.jestch.2015.07.011

Shahi, Md. N. S., Orka, N. A., & Ahmed, A. (2024). 2DOF-PID-TD: A new hybrid control approach of load frequency control in an interconnected thermal-hydro power system. *Heliyon*, *10*(17), e36753. https://doi.org/10.1016/j.heliyon.2024.e36753

Shrestha, A., & Gonzalez-Longatt, F. (2021). Frequency Stability Issues and Research Opportunities in Converter Dominated Power System. *Energies*, *14*(14), 4184. https://doi.org/10.3390/en14144184

So, G.-B. (2021). A Modified 2-DOF Control Framework and GA Based Intelligent Tuning of PID Controllers. *Processes*, *9*(3), 423. https://doi.org/10.3390/pr9030423

So, G.-B. (2022). Design of Linear PID Controller for Pure Integrating Systems with Time Delay Using Direct Synthesis Method. *Processes*, *10*(5), 831. https://doi.org/10.3390/pr10050831

Veerasamy, V., Abdul Wahab, N. I., Ramachandran, R., Vinayagam, A., Othman, M. L., Hizam, H., & Satheeshkumar, J. (2019). Automatic Load Frequency Control of a Multi-Area Dynamic Interconnected Power System Using a Hybrid PSO-GSA-Tuned PID Controller. *Sustainability*, *11*(24), 6908. https://doi.org/10.3390/su11246908

Verma, R., Gawre, S. K., Patidar, N. P., & Nandanwar, S. (2024). A state of art review on the opportunities in automatic generation control of hybrid power

system. *Electric Power Systems Research*, *226*, 109945. https://doi.org/10.1016/j.epsr.2023.109945

Vorobev, P., Greenwood, D. M., Bell, J. H., Bialek, J. W., Taylor, P. C., & Turitsyn, K. (2019). Deadbands, Droop, and Inertia Impact on Power System Frequency Distribution. *IEEE Transactions on Power Systems*, *34*(4), 3098–3108. https://doi.org/10.1109/TPWRS.2019.2895547

Wadi, M., Shobole, A., Elmasry, W., & Kucuk, I. (2024). Load frequency control in smart grids: A review of recent developments. *Renewable and Sustainable Energy Reviews*, *189*, 114013. https://doi.org/10.1016/j.rser.2023.114013

Wang, X., & Lu, N. (2024). Alleviating imbalanced problems of reinforcement learning when applying in real-time power network dispatching and control. *Expert Systems with Applications*, *255*, 124730. https://doi.org/10.1016/j.eswa.2024.124730

Yang, D., Yan, G.-G., Zheng, T., Zhang, X., & Hua, L. (2022). Fast Frequency Response of a DFIG Based on Variable Power Point Tracking Control. *IEEE Transactions on Industry Applications*, *58*(4), 5127–5135. https://doi.org/10.1109/TIA.2022.3177590

Zhao, S., Zhang, T., Ma, S., & Chen, M. (2022). Dandelion Optimizer: A nature-inspired metaheuristic algorithm for engineering applications. *Engineering Applications of Artificial Intelligence*, *114*, 105075. https://doi.org/10.1016/j.engappai.2022.105075

Zhou, J., Jia, Y., Yong, P., Liu, Z., & Sun, C. (2024). Robust deep Koopman model predictive load frequency control of interconnected power systems. *Electric Power Systems Research*, *226*, 109948. https://doi.org/10.1016/j.epsr.2023.109948